



Intra-annual stem radial increment patterns of Chinese pine, Helan Mountains, Northern Central China

Jiani Gao^{1,2} · Bao Yang¹ · Minhui He^{1,3} · Vladimir Shishov^{4,5}

Received: 22 August 2018 / Accepted: 12 January 2019 / Published online: 6 February 2019
© Springer-Verlag GmbH Germany, part of Springer Nature 2019

Abstract

Key message We investigate the intra-annual growth patterns of Chinese pine in Helan Mountains, confirming that regional water status plays a dominated role in stem radial increment.

Abstract The associations between environmental conditions and stem radial increment (SRI) are useful for assessing a species' growth response to climate change. Intra-annual SRI dynamics of Chinese pine (*Pinus tabulaeformis*) were monitored half-hourly by automatic point dendrometer during the growing season (May–September) in 2016 and 2017 at two altitudes in the Helan Mountains, northern central China. Here, we compared the seasonal growth patterns between two altitudes and 2 years. Trees at low altitude are characterized by earlier cessation, shorter growing season, and lower growth rate, resulting in less annual growth, which may reflect the greater drought intensified by rising temperature at low altitude. June precipitation significantly affected tree growth rate. The xylem growth was active when daily mean air temperature was 9.9 °C at our study region for *P. tabulaeformis* in an arid environment. During the growing season, daily stem radial increment showed a significantly positive correlation with precipitation and a negative correlation with daily air temperature at all altitudes. Climatic variables associated with tree water status, namely precipitation, vapor pressure deficit, and relative humidity, played important roles in daily stem radial increment as the same result as a linear mixed model. These factors drive the complex physiological processes of stem radial increment by influencing the moisture available to the tree.

Keywords Stem radial increment · Dendrometer · V–S model · *Pinus tabulaeformis* · Seasonal patterns · Helan Mountains

Communicated by E. Liang.

✉ Jiani Gao
gaojiani@lzb.ac.cn

- ¹ Key Laboratory of Desert and Desertification, Northwest Institute of Eco-Environment and Resources, Chinese Academy of Sciences, Lanzhou 73000, China
- ² University of Chinese Academy of Sciences, Beijing 10048, China
- ³ Institute of Geography, University of Erlangen-Nürnberg, 91058 Erlangen, Germany
- ⁴ Mathematical Methods and Information Technology Department, Siberian Federal University, 660075 Krasnoyarsk, Russia
- ⁵ Laboratory of Tree-Ring Structure, V.N. Sukachev Institute of Forest, Siberian Branch of the Russian Academy of Sciences, 660036 Krasnoyarsk, Russia

Introduction

Chinese pine (*Pinus tabulaeformis*) is an endemic, wide-spread, cold- and drought-resistant conifer species in northern China. It has been extensively used for dendroclimatic studies (Li et al. 2007; Liang et al. 2009; Liu et al. 2004; Sun and Liu 2015; Zeng et al. 2018), revealing that tree-ring width in Chinese pine is largely controlled by regional moisture conditions. In particular, Li et al. (2007) presented a drought reconstruction (Palmer drought severity index) for March–July during AD 1788–1999 in the Helan Mountains, northern central China. To gain a detailed understanding of the relationships between Chinese pine growth physiology and environmental and climatic signals in the Helan Mountains, clearer and biologically relevant climatic information recorded in intra-annual tree growth is required.

The automatic dendrometer is an efficient instrument with which to continuously monitor stem radius changes at time scales ranging from seconds to days, and is crucial to understand the tree's response to environmental conditions

over short time scales (Deslauriers et al. 2007). Dendrometers are now widely used in quantifying and dating the seasonal process of wood formation (Mäkinen et al. 2008) and describing seasonal tree growth patterns (Maaten 2013b), yet most studies have focused on exploring the association between tree growth and climate conditions (Bouriaud et al. 2005; Deslauriers et al. 2003; Duchesne et al. 2012; King et al. 2013; Wang et al. 2015). Response of tree growth to climatic condition has not been directly assessed (Schweingruber 1996). By combining tree growth with synchronous stem radial increment estimates may provide detailed information on inter-annual dynamics. Indeed, daily stem radial increment (SRI) are mainly determined by transpiration and soil water content (Bouriaud et al. 2005), especially in semi-arid and arid areas (Zhang et al. 2016b). Gruber et al. (2009) found that daily variations of *Pinus cembra* (L.) were positively correlated with tree water status (precipitation and relative humidity) in the alpine eco-tone. Likewise, daily SRI were correlated with the maximum daily vapor pressure deficit in Ecuador (Bräuning et al. 2009). Liu et al. (2017) argued that soil moisture was the main factor limiting the stem radial variation during the growing season in Northwest China's semi-humid climate. In the growing season, changes in radial growth of Schrenk spruce (*Picea schrenkiana* Fisch. et Mey) were positively correlated with daily precipitation and relative humidity in the Tianshan Mountains (Zhang et al. 2016b). The effects of environmental and climatic signals on intra-annual stem radial growth and the seasonal growth patterns of Chinese pine remain unclear.

The onset of tree stem radial growth is a crucial variable when exploring the response of tree growth to climate conditions. Several studies using the 'micro-core' method have found that temperature is a critical factor controlling growth activity in cold climates (Li et al. 2013, 2017; Rossi et al. 2008). Rossi et al. (2008) found a daily mean air temperature for xylogenesis of 8–9 °C in seven conifer species in cold environments; Gruber et al. (2010) noted that air temperature at the onset of growing season exceeded the long-term mean by 6.4 °C in April, 2007 in Scots pine. Temperature and precipitation thresholds for the onset of xylogenesis in Qilian juniper have also been assessed (Ren et al. 2017). To gain a deeper insight into the respective roles of climatic variables on intra-annual radial growth of Chinese pine, it is crucial to identify any temperature-limited growth relationship in Chinese pine and to determine the onset of tree growth.

This paper examines the seasonal growth patterns at two different altitudes and discusses the critical climate factors that affect daily stem radial increment. The objectives are: (i) to compare the intra-annual stem radial increment patterns between different altitudes; (ii) to describe the growth–climate relationships using a linear mixed model; and (iii) to identify if there is a temperature threshold for the onset of growth in this region.

Materials and methods

Study site

This study was conducted in Suyukou National Forest Park (SYK, Yinchuan, Ningxia Hui Autonomous Region), located in the eastern Helan Mountains (38°44'N, 105°54'E), northern central China. The site lies at the geographical boundaries between the arid and semi-arid area as well as between the monsoon and non-monsoon regions. The canopy vegetation is dominated by Chinese pine (*P. tabulaeformis*) at 1900–2350 m a.s.l. The average annual precipitation varies from 200 to 600 mm between the valleys and summits; the annual mean temperature is 8.4 °C; mean temperatures in January and July are about −7.8 °C and 21.9 °C, respectively. During the study period, the precipitation between May and September was 450 mm and 300 mm in 2016 and 2017, respectively, and accounted for over 80% of the total annual precipitation; the mean annual temperatures were 5.76 °C and 5.68 °C in 2016 and 2017, respectively. Two sites were selected at two altitudes: 2330 m a.s.l. (the upper altitude of Chinese pine growth in this region) and 2010 m a.s.l., labeled as SPH and SPL.

Dendrometer measurements

A total of ten healthy and upright Chinese pines, without apparent injuries or defects, were selected and instrumented from May 16, 2016 to 2017 with automatic high-resolution point dendrometers (Ecomatik, Germany; type DR; with ± 2 μm precision), at 1.0–1.3 m height, to continuously monitor tree growth. The outermost dead bark was removed without wounding the cambial zone to reduce the influence of contraction and expansion of bark. The point dendrometer converts stem radius changes to an electrical signal, which is recorded every 30 min with a data logger (DL18, accuracy $\pm 0.1\%$). Tree-ring widths and age were determined in the laboratory, where widths were measured to a precision of 0.001 mm. Due to environmental or instrumental problems, some measurements did not cover the complete growth season. A summary of trees included in the study is shown in Table 1.

Meteorological measurements

Two automated weather stations (HOBO U30, USA) were installed at an open, relatively flat area 50 m away from the sample trees, and were constantly monitoring meteorological conditions during the same time period as that of the dendrometer measurements at both altitudes. Measurements included air temperature (T , °C), precipitation (Prep, mm), relative

Table 1 Summary of biological characteristics of sample trees

Tree no.	2016	2017	Height (m)	DBH (cm)	Age (year)
SPL01	*		7.2	79	98
SPL02	*	*	4.8	60	96
SPL03	*	*	6.9	61	107
SPL07	*	*	9.8	59	92
SPH02	*	*	7.2	72	69
SPH03	*	*	9.7	66	67
SPH06	*	*	8.3	61	60

Asterisk denotes trees recorded in the study

humidity (RH, %), soil temperature, and soil water content at 20 cm depth (TS20, °C; SWC20, m³/m³). The vapor pressure deficit (VPD, KPa) was calculated from RH and mean air temperature following the Magnus equation (Murray 1967). All meteorological data were recorded every 30 min.

Data analysis

SRI comprises an irreversible component (due to growth) and a reversible component (due to changes in the water balance of stem tissues) (Irvine and Grace 1997). Thus, the observed stem changes are determined by: (1) stem growth arising from new layers of woody cells; (2) water-related swelling and shrinking of elastic tissues located mainly in the bark (Zweifel and Hasler 2000; Zweifel et al. 2005). The raw half-hourly dendrometer data were processed to extract daily SRI, following two main approaches: (1) the daily approach, which involves calculating the diurnal cycle characteristics (i.e., daily maximum, minimum, and mean) (Bouriaud et al. 2005; King et al. 2013; Maaten et al. 2013a); (2) stem-cycle approach, in which the stem radius changes contain three distinct phases: the contraction phase, expansion phase, and stem radius increment phase (Deslauriers et al. 2003). Time series based on the daily and stem-cycle approaches are strongly correlated (Deslauriers et al. 2007), and we chose daily maximum values of the dendrometer record to extract daily SRI for further analysis by calculating the difference between maximum values of 2 consecutive days for each trees and consider daily SRI value as zero when negative values occurred.

We calculated the average SRI of Chinese pines at the SPH and SPL sites. We described the dynamics of tree growth using the sigmoid Gompertz function (Camarero 1998; Duchesne et al. 2012; Wang et al. 2015), defined as follows:

$$Y = Y_0 + A \exp[-e^{(\beta - \kappa t)}],$$

where Y is daily stem radius change; Y_0 and A are the lower and upper asymptotes, respectively; β is the x -axis placement parameter; κ is the rate of change parameter; t is the day of year (DOY). Timing of growth onset and cessation is thus defined as the DOY when modeled daily growth rates passed the threshold of 4 $\mu\text{m}/\text{day}$. To aid comparison, the period from May to September was selected as an approximate growth period, with May 16 in 2016 and May 1 in 2017 arbitrarily set to zero (0) for all point dendrometers (Tardif et al. 2001). The goodness of fit of the non-linear regression equation is defined as follows:

$$R_{\text{new}} = 1 - \sqrt{\sum (y - y^*)^2 / \sum y^2},$$

where y and y^* are the observed and modeled stem radius variations, respectively.

The Vaganov–Shashkin (V–S) model is used to simulate the non-linear response of tree growth to climate factors. In this model, it was assumed that the seasonal tree growth depended on three main factors: solar irradiation, temperature, and water content in soil (Vaganov et al. 2006). The daily cambial cell production is, thus, determined by these three main factors. Here, we used an updated tree-ring physiological VS procedure (VS oscilloscope, <http://vs-genn.ru/downloads/>) (Shishov et al. 2016) to model tree-ring width series, as well as the onset and cessation DOY of Chinese pine during the period of 1951–2017 at our study sites. The chronology that we used extended from 1904 AD to 2017 AD and comprised 83 cores from 48 Chinese pines in SYK, at elevations of 1900–2400 m a.s.l. Meteorological data were obtained from the nearby meteorological station in Yinchuan (1110.9 m a.s.l.). We adjusted the daily climate station data by -6.6 °C (equivalent to an altitude of 2250 m a.s.l.) prior to their use as the model input data. The parameters used in the VS oscilloscope model are shown in Table 2.

We used logistic regression to calculate the probability of tree growth commencing at a given temperature. Binary responses were coded as growth (value 1) or non-growth (value 0). The logistic regression is defined as follows:

$$\text{Logit}(\pi_x) = \ln\left(\frac{\pi_x}{1 - \pi_x}\right) = \beta_0 + \beta_1 x_j,$$

where π_x is the probability of tree growth commencing; β_0 and β_1 are the intercept and slope of the logit regression, respectively; x_j is the temperature on day j . When $\pi_x = 0.5$, $\text{Logit}(\pi_x) = 0$, and $x = -\beta_0/\beta_1$ is the temperature threshold

Table 2 Summary of VS oscilloscope model parameter setting

Parameter	T_{min}	T_{opt1}	T_{opt2}	T_{max}	W_{min}	W_{opt1}	W_{opt2}	W_{max}	T_{beg}	D_{root}	K_1	K_2	K_3
Value	10	13	24	30	0.1225	0.375	0.45	0.6	100	500	0.5	0.095	0.045

for growth. For a temperature over x , the tree was more likely to be growing than not growing (Rossi et al. 2007).

As the focus of our analysis is the growth trends during the active growing period (May–September), we used Pearson correlation and a linear mixed model [LME; *nlme* packages; (Pinheiro and Bates 2001)] to describe the relationships between climatic variables with the strongest significant correlations and stem radial increment at two altitudes and individual levels, respectively. A LME was established for both SPH and SPL in 2016 and 2017, using daily climatic variables as fixed effects, and characteristics of individual trees nested within the 2 years as random effects. The LME is defined as follows:

$$\text{SRI}_i = X_i\beta + Z_iB + \varepsilon_i.$$

Here, SRI_i represents stem radius increments for individual tree i ; X and Z represent fixed effects (daily climatic variables and environmental variables) and random effects (tree individuals, year), respectively; β and B are the vectors of fixed effects and random effects, respectively; ε is the error vector. We used graphical inspection of the standard residual and fitted values to evaluate the goodness of fit of the LME. We selected the fixed effects using a log-likelihood ratio, and then tested the site-level and tree-level significance of

random effects on all the selected climate variables (Lapointe-garant et al. 2010). The Akaike information criterion (AIC) was used to weight the complexity of the estimated models along with the superiority of the model fitting data. All analyses were performed using the R statistical environment (R Core Team 2012).

Results

Climate variables during the growing period

The study area had a typical continental climate characterized by warm-wet summers and cold-dry winters (Fig. 1). During the growing period (May–September), the daily mean air temperature during 2016–2017 reached 14 °C and 16.5 °C, respectively at SPH and SPL (Fig. 1a, b). There was more precipitation in 2016 (over 500 mm) than in 2017 (396.12 mm), and notably extreme rainfall in August 2016 contributed 297.54 mm. In June 2017, the precipitation was slightly higher than that in 2016 (Fig. 1c, d). The altitudinal temperature and precipitation trends were apparent, decreasing and increasing with the greater altitude, respectively.

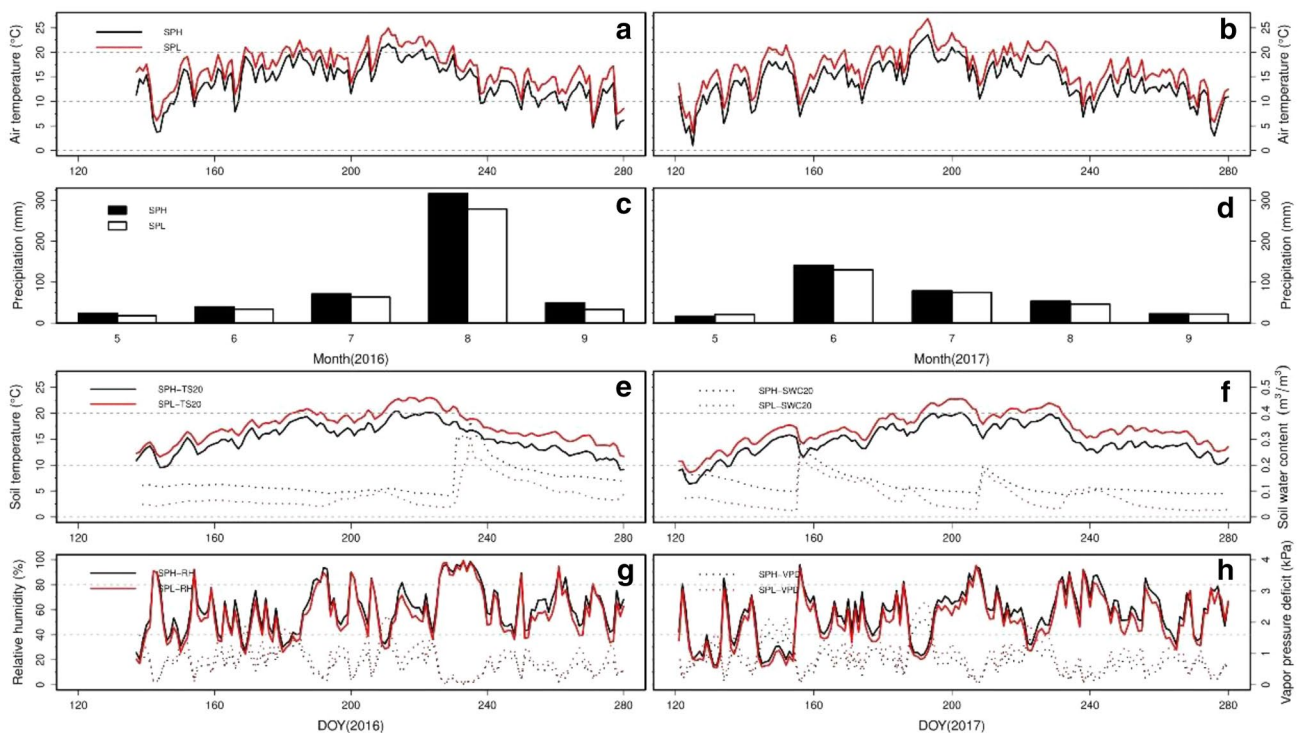


Fig. 1 Climatic records from May to September in 2016 and 2017. Mean daily air temperature recorded at sites SPH and SPL (a, b). Monthly precipitation totals at both sites (c, d). Mean daily soil temperature at 20 cm depth (lines) and mean daily soil water content at

20 cm depth (dotted lines) at SPH (black) and SPL (red) (e, f). Relative humidity (lines) and vapor pressure deficit (dotted lines) at SPH (black) and SPL (red) (g, h)

During the study period, soil temperature at 20 cm depth was over 5 °C, and 0.5 ± 0.2 °C higher than the mean air temperature. The average soil water contents at 20 cm depth, at SPH and SPL, were $0.14 \text{ m}^3/\text{m}^3$ and $0.083 \text{ m}^3/\text{m}^3$ in 2016, and $0.12 \text{ m}^3/\text{m}^3$ and $0.075 \text{ m}^3/\text{m}^3$ in 2017, respectively. Trends in soil temperature and soil water content with altitude were evident (Fig. 1e, f). Relative air humidity ranged from 15 to 96%, and the vapor pressure deficits ranged from 0.02 to 2.62 kPa (Fig. 1g, h).

Seasonal growth patterns and altitudinal trend

Observed stem radius variation (SRV) in 2 years is plotted in Fig. 2. Differences in tree growth between SPH and SPL were evidently greater in 2016 than in 2017. Growth amounts of Chinese pine in 2017 were higher than in 2016, and the individual differences in growth during 2017 are evident.

Results simulated using the Gompertz function are shown in Fig. 3. The goodness of fit of the Gompertz function, R_{new} , indicated that the non-linear regressions accounted for 80–97% of variability in the dendrometer measurements. Model results for 2016 showed that the onset of the growing season was around 19 May (DOY 140) at SPH and from 20 May to early June (DOY 138–160) at SPL; the cessation day was around 1 September (DOY 245) at SPH, and ranged from early August to late August at SPL. In 2017, the onset of the growing season was from 3 to 25 May (DOY 124–145) at SPH, and from 10 to 27 May (DOY 130–147) at SPL; the cessation day was from 15 August to 6 September (DOY 210–250) at SPH, and from 14 July to 21 August at SPL.

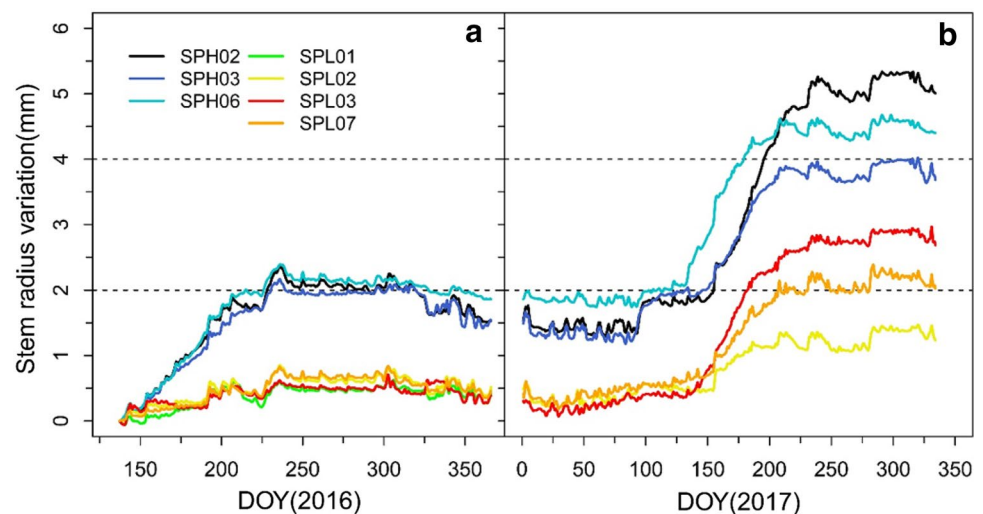
The main growing seasons were DOY 140–246 and DOY 135–230 at SPH, and DOY 148–232 and DOY 137–213 at SPL, in 2016 and 2017 respectively, as indicated by dendrometer records. Trees in 2017 were

characterized by an earlier onset and cessation DOY, and resulted in a shorter growth period. As the first dendrometer record was collected on DOY 137 in 2016, when three trees had started to grow; thus, the onset day of tree growth could not be clearly identified in 2016 and the error would be within 3 days. Cumulative growth was 0.4 ± 0.05 mm at SPH and 0.2 ± 0.05 mm at SPL in 2016, compared with 0.6 ± 0.2 mm and 0.4 ± 0.15 mm at SPH and SPL in 2017 (Fig. 3). The average seasonal growth patterns at SPH and SPL site are shown in (Fig. 4). The individual growth differences are evident in 2017. The average stem radius variations at the SPH and SPL sites were 16.80 ± 1.09 $\mu\text{m}/\text{day}$ and 4.38 ± 0.83 $\mu\text{m}/\text{day}$ in 2016, and 18.21 ± 5.68 $\mu\text{m}/\text{day}$ and 11.14 ± 6.15 $\mu\text{m}/\text{day}$ in 2017, indicating that both SPH and SPL sites exhibited high growth rates and high growth variability between individual trees in 2017. The timings of maximum growth rates were similar at SPH and SPL in 2 years, both being around 170 ± 15 DOY, corresponding to mid-June.

V–S model simulation results

We found a significant agreement between the observed and V–S model simulated chronologies with a correlation coefficient of 0.602 (Fig. 5a, $p < 0.001$). The minimum daily mean air temperature for tree growth was 10.0 °C. Tree growth phenology showed a slightly advancing trend in the onset day, whereas the cessation of growth remained unchanged. In general, the average main growth period for Chinese pine in the study area during 1951–2017 was from DOY 135 ± 15 to DOY 254 ± 10 according to the V–S model results. The average onset and cessation days were about DOY 135 and DOY 254, respectively, equivalent to an average growth duration of 119 days.

Fig. 2 Observed stem radius variation. Dendrometer raw measurements from May 15, 2016 to November 30, 2017



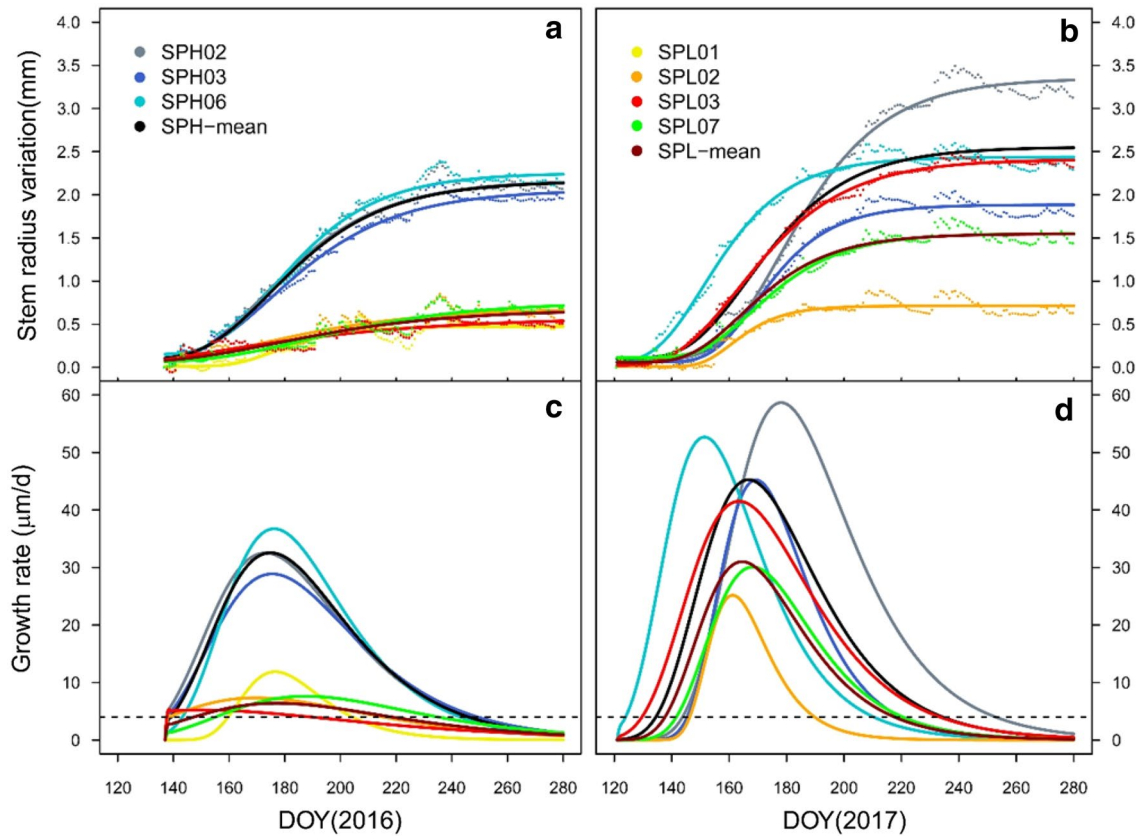


Fig. 3 Observed and modeled stem radius variation at SPH and SPL. Dendrometer raw measurements (dots) and the Gompertz function modeled curves (lines) from May to September in 2016 and 2017 (a,

b), modeled growth rates in 2016 and 2017 (lines) (c, d). The dotted lines (c, d) represent daily growth rates equal to 4 µm per day

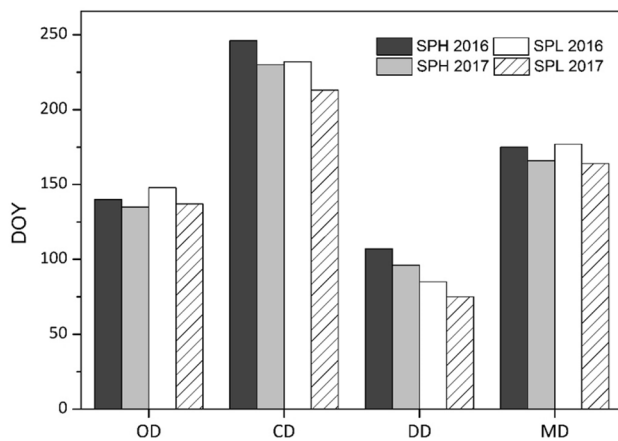


Fig. 4 Characterization of the seasonal growth patterns during the active growing period. OD, CD, DD, and MD represent the onset DOY, cessation DOY, growing season duration (days), and day of maximum growth rate, respectively

Threshold temperatures

We calculated the average threshold temperatures for which there was a probability of 0.5 of tree growth onset during 2016–2017 at SPH and SPL (Fig. 6). At SPH, the average thresholds for minimum, mean, and maximum air temperature and mean soil temperature at 20 cm depth were 4.84 ± 0.94 °C, 9.90 ± 1.00 °C, 15.50 ± 1.11 °C, and 11.73 ± 0.85 °C ($p < 0.05$). The respective threshold temperatures at SPL were 7.88 ± 1.44 °C, 12.42 ± 1.58 °C, 16.80 ± 1.87 °C, and 13.95 ± 0.88 °C ($p < 0.05$), and, therefore, significantly higher than those at SPH (Paired t test, $p < 0.001$). The mean air temperatures during the tree growth period were 9.7 ± 0.1 °C and 13.23 ± 0.7 °C at SPH and SPL, respectively. No significant differences were found between 2016 and 2017 for the onset of tree growth.

The relationship between SRI and climate variables

Throughout the two growing seasons in 2016 and 2017, the Pearson correlation coefficient was used to quantitatively describe the relationship between climatic variables

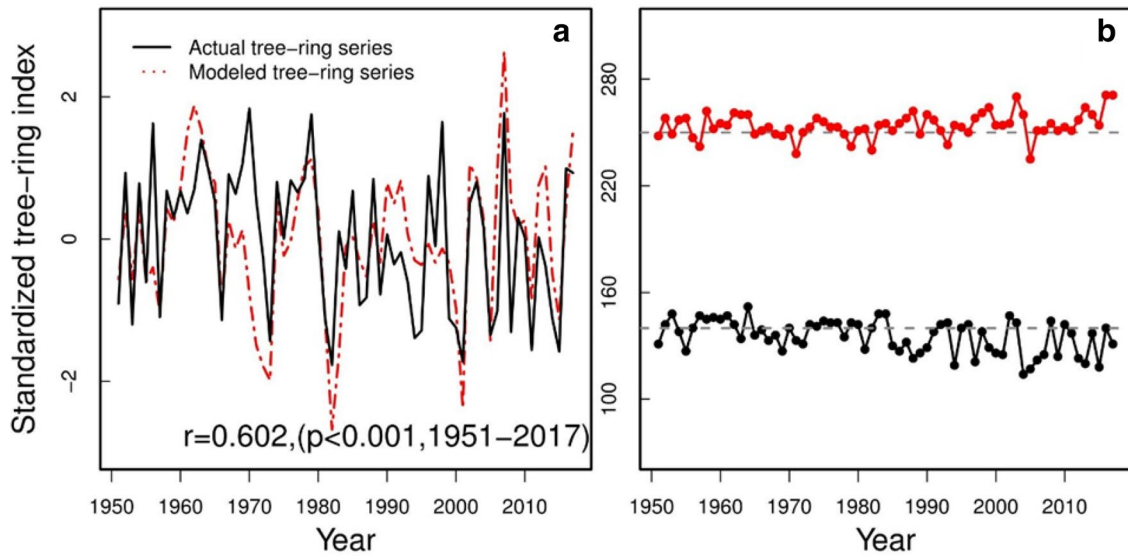


Fig. 5 Actual and modeled tree-ring series (a), and their derived onset (black lines) and cessation day of year (red lines) of tree growth (b) during the period of 1951–2017

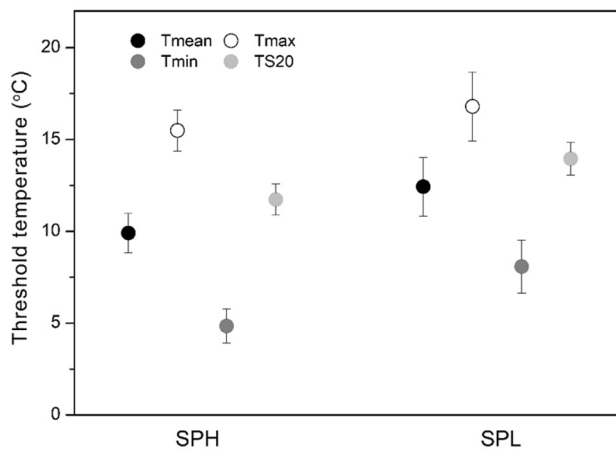


Fig. 6 Threshold mean, maximum, minimum air, and mean soil temperatures at 20 cm depth corresponding to the 0.5 probability of active growing at SPH and SPL during 2016–2017. Error bars indicate the standard deviation among trees

and SRI. The SRI-climate response patterns were similar at SPH and SPL.

Monthly correlation analysis (Fig. 7) between SRI, temperature, and precipitation showed a clearly opposite response. For the whole growing season in both years, temperature showed a significant negative correlation with daily SRI. The minimum temperature at May at SPH and SPL in both 2016 and 2017 showed a positive effect to daily SRI, as well as at August in 2016 at both sites. In general, precipitation exhibited a positive relationship with

daily SRI, especially in August 2016, and precipitation was positively related with daily SRI.

For the whole growing season (Fig. 8), daily SRI showed significantly positive correlations with Prep and RH, whereas VPD was significantly negatively correlated with daily SRI. Moreover, T_{mean} , T_{max} , and T_{min} were negatively associated with daily SRI, except for a few trees, whereas TS20 showed a positive relationship with daily SRI. SWC20 showed opposite effects on daily SRI during the two years. All results indicated that wet and cool summer conditions enhanced tree growth at both SPL and SPH.

The final LME formula which we used was as follows:

$$SRI = T_{max} + Prep + TS20 + SWC20 + RH + VPD + Altitude.$$

Fixed effects included every climatic variable [T_{max} ($p < 0.01$), Prep ($p < 0.001$), TS20 ($p < 0.01$), SWC20 ($p < 0.001$), RH ($p < 0.01$) and VPD ($p < 0.01$)], environment variable [Altitude ($p < 0.001$)], and interactive effects between all climatic variables. We had random intercept for trees and by-year and by-age random slopes to reduce the potential loss of ecological signals derived from growth variability among trees. p values were obtained by likelihood ratio tests of the full model with the effect in question against the model without the effect in question. The final formula explained an average 51% of the variance in daily SRI across time and sites and the correlation coefficient between observed daily SRI and predicted SRI was 0.82 ($p < 0.001$). The fitting results demonstrated that the precipitation and soil water content acted as dominant climatic drivers, at both sites and in both years. Modeling results show that SRI is mainly driven by Prep, RH, VPD, and altitude,

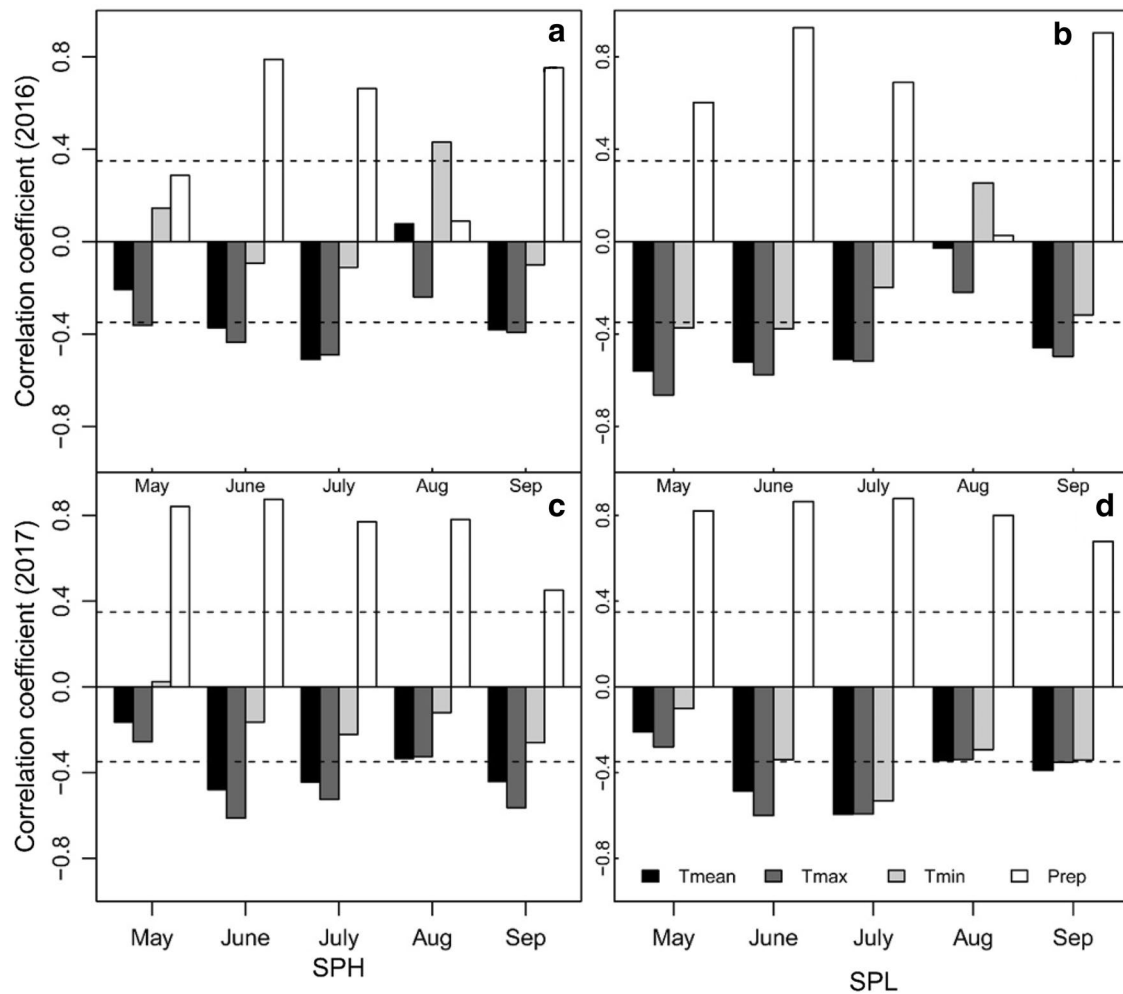


Fig. 7 Monthly Pearson correlation coefficient between daily SRI and climatic variables (daily mean temperature, maximum temperature, minimum temperature, and precipitation) from May to September in

2016 (**a, b**) and 2017 (**c, d**) at SPH (**a, c**) and SPL (**b, d**). The dotted lines indicate the 0.05 significant level

and interactive influences between the above climate variations seem particularly important. The model accurately simulates the growth trend due to climatic factors. LME has been demonstrated to be a suitable technique for modeling SRI and merits further research.

Discussion

Stem variation and its seasonal patterns

Temperature can influence both production and differentiation (Deslauriers and Morin 2005), and determines the onset of growth and other wood formation process (Moser et al. 2010; Yang et al. 2017). We found the onset DOY was 5 days and 10 days earlier, respectively, at SPH and SPL in 2017 than in 2016 (Fig. 4). The mean temperature

in May 2017 (mean value of two altitudes, 15.58 °C) was slightly higher than that in 2016 (12.12 °C) (Fig. 1). It can be inferred that temperature is a key driver that limits the onset of tree growth. According to Körner and Paulsen (2004), there is a mean air temperature threshold of 5–8 °C at tree-line positions worldwide. In this study, the Chinese pines begin to grow when the daily mean air temperature was 9.9 °C at SPH, in 2016 and 2017. The V–S model simulation also showed that the minimum daily mean air temperature for tree growth was 10 °C. Xylogenesis was active when daily mean air temperature was 10.1 °C for Scots pine (*Pinus sylvestris* L.) in Alpine valley (47°14'00" N, 10°50'20" E) (Swidrak et al. 2011). Overall, our results support the xylem growth which was active when daily mean air temperature was 9.9 °C at our study region for *P. tabulaeformis* in an arid environment, which can control the growing season of Chinese pine.

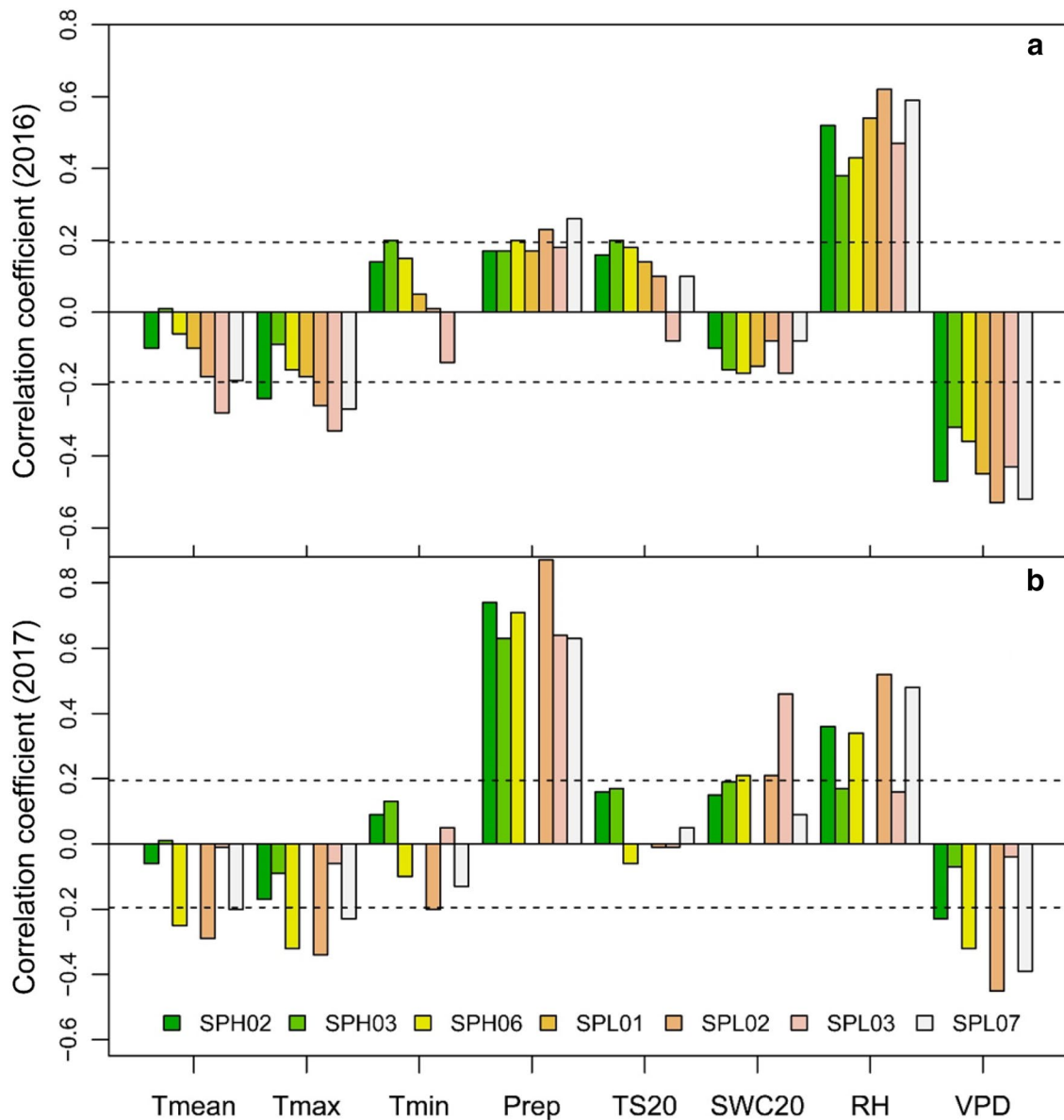


Fig. 8 Pearson correlation coefficient between daily SRI for individual trees and all climatic variables during the whole growing season in 2016 (a) and 2017 (b) for every trees. The dotted lines indicate the 0.05 significant level

The maximum growth rate occurred in mid-June. Rossi et al. (2006) demonstrated that the maximum growth rate occurred around the time of maximum day length (Summer Solstice) connected with maximum photoperiod in Italy. Growth rate variability during the growing season was greater in 2017, especially after rainfall events. Several studies have demonstrated that moisture is the main factor limiting the stem radius variation during the growing season in semi-arid, arid, and even semi-humid regions in China (Liu et al. 2017; Zhang et al. 2016b). During the main growing season of June and July, discrete rainfall were more evident in 2017 than in 2016, and the precipitation in 2017

(212 mm) was greater than in 2016 (104 mm). The precipitation caused a large fluctuation in water content, leading directly to a faster growth rate. We argue that this largely reflects a combination of water status.

In this study, we found that the onset day was roughly similar at SPH and SPL site, whereas the cessation day was around 2–3 weeks earlier at SPL site compared with SPH site. Moreover, a previous study demonstrated that radial growth of Chinese pine showed significantly decreased trend at low altitude (2032 m a.s.l.), whereas the growth trend remained almost steady at high altitude (2361 m a.s.l.) during the past decades on the eastern Helan Mountains (Zhang

et al. 2016a). The mean temperature of growing season (May–September) showed significant increasing trend during the period of 1953–2018, whereas the total precipitation kept unchanged (Fig. 9). As the SPL site had higher temperature and lower precipitation, trees at SPL were more vulnerable to the increasing temperature. Thus, intensified drought due to rising temperature may result in radial growth reduction and earlier growth cessation at low altitude.

In general, the durations of growth at SPH and SPL were 100 days and 80 days in 2016–2017, which are longer than those of Qinghai spruce (*Picea crassifolia*) (Tian et al. 2017) and Qilian juniper (Wang et al. 2015) in the Qilian Mountains, possibly due to the higher air temperature in our study region. There was no difference observed in the onset of the tree growth period between the two altitude classes (*t* test, $p < 0.05$). Compared with SPL, trees at SPH were characterized by a later cessation growth period, longer duration of growing season, and higher growth rate, resulting in a higher amount of growth. Evident differences in stem seasonal growth across altitudinal gradients were observed in Chinese pine (*t* test, $p < 0.001$), in apparent contradiction to the study of Qilian juniper in northwestern China (Wang et al. 2015); this confirms that growing season duration decreased with altitude.

Impact of climate on the daily SRI

The water and heat requirements of trees vary between the different phases of tree growth. In the monthly correlation patterns (Fig. 7), we found a strictly positive relationship between precipitation and SRI, especially at June, when the maximum growth rate occurred. Temperature was mainly negatively correlated to SRI. Minimum air temperature in May was positively related to SRI, which may indicate that a reasonable heat level will promote the growth of Chinese pine in the early growing season. There was a

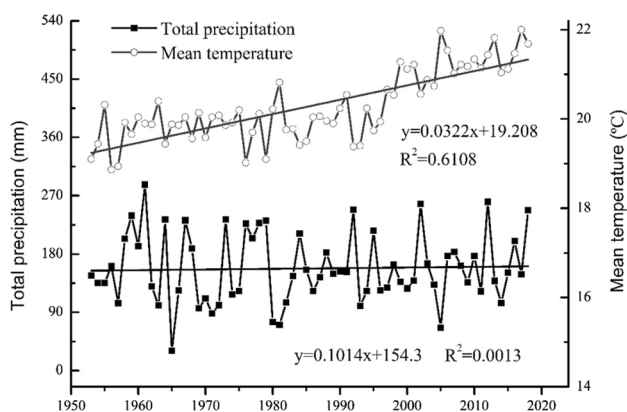


Fig. 9 Climate trends of growing season (May–September) during 1953–2018 in Yinchuan climate station

positive correlation between minimum air temperature and SRI, since temperature dropped significantly following a sustained heavy rainfall period in August 2016. During the main growth period, we found that the effects of climate variations associated with water status of the tree on daily SRI of Chinese pine were generally high. This is because the moisture conditions limit the enlargement of cambial cells, regarded as the primary drivers of daily radial variations (Deslauriers et al. 2003). We found that the precipitation and relative humidity (RH) were significantly positively correlated with daily SRI and, conversely, there was a significant negative correlation between the vapor pressure deficit (VPD) and daily SRI (Fig. 8). These strong correlations could be explained by transpiration rates and SRI is thus dependent on hydrothermal regime (Vieira et al. 2013). Several studies have found that radial growth in Qinghai spruce is positively related to RH and precipitation both on the northeastern Tibetan Plateau (Liang et al. 2006) and in the Qilian Mountains (Wang et al. 2016), China. We infer that, during rainy days, the wet crown has a decreased leaf water potential, which, in turn, enlarges the xylem cells (Zweifel et al. 2006) and thus results in the radial growth of trees. The main physiological effect of VPD is to limit cell enlargement and growth owing to its indirect effect on cell turgor pressure (Major and Johnsen 2001), further confirming that water status is a critical factor to SRI.

We found a positive effect of T_{\min} on SRI at SPH. Cell growth is assumed to occur mainly during night (Hosoo et al. 2002; Li et al. 2013), early morning, or rainy days (Urrutia-Jalabert et al. 2015) when temperature is low. Deslauriers and Morin (2005) reported that daily growth responses in conifers at high latitude were related to T_{\min} . Li et al. (2013) also argued that T_{\min} positively influences wood formation in Smith fir on the southeastern Tibetan Plateau. In addition, a positive correlation was also observed between TS20 and SRI, because warmer soil temperatures positively influenced stem rehydration, root water uptake, and the consequent beneficial effect on internal water balance (Urrutia-Jalabert et al. 2015).

We captured an extreme continuous rainfall during August 21–23 in 2016, where cumulative precipitation reached 200 mm concentrated in Aug. 23 7:00 p.m. to Aug. 24 9:00 a.m. (Fig. 10c, d). SRI showed a continuous positive variation (Fig. 10a, b), the maximum SRI preceded the maximum hourly precipitation, indicating that SRI in Chinese pine slows to growth when the tree water status reaches saturation. Since the extreme continuous rainfall occurred at the end of growth season, SRI did not show correspondingly continuous positive values when the rain eased off. Soil water content increases after significant precipitation (> 10 mm), thus promoting radial growth by improving water status and cambial cell turgor in the stem (Jiang et al. 2015). The automatic dendrometer can monitor the

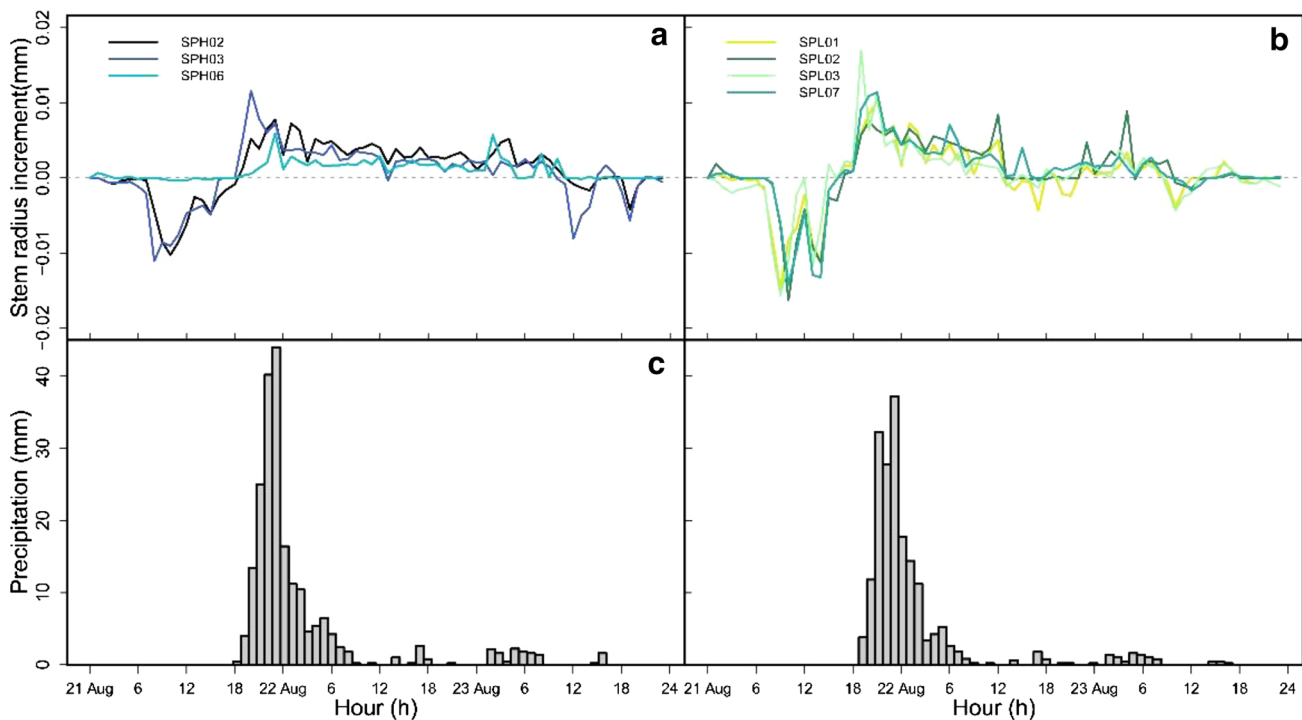


Fig. 10 An extreme continuous rainfall event during 21–23 August, 2016 at SPH (c) and SPL (d), and the corresponding SRI (a, b)

dynamics of stem radial variations under climate variations in great detail.

Conclusions

This work compared the intra-annual patterns of stem radial increment of Chinese pine, at two elevations, in 2016 and 2017, in an arid area of northern central China. The main growing season was DOY 140–246 and DOY 135–230 at SPH, and DOY 148–232 and DOY 137–213 at SPL, in 2016 and 2017, respectively. We found that Chinese pines begin to grow when the daily minimum, mean, and maximum temperatures are 4.84–7.88 °C, 9.90–12.42 °C, and 15.50–16.80 °C, respectively, in this arid environment. The climate-growth patterns are similar at different altitudes. Considering the short time scales, the climate variables associated with water status showed significantly positive/negative associations with SRI, reflecting the positive effects of water on stem water potential and especially stem increment during the growth period.

Author contribution statement BY conceived the ideas; BY and JNG designed the study; JNG performed the statistical analysis and wrote the first draft of the manuscript; MHH and VS contributed to the writing of this manuscript. All authors contributed to the manuscript.

Acknowledgements This study is supported by the National Nature Science Foundation of China (Grants: 41520104005, 41325008), and the Belmont Forum and JPI-Climate Collaborative Research Action ‘INTEGRATE’ (Grant: 41661144008). VS was supported by the Ministry of Education and Science of the Russian Federation (Project # 5.3508.2017/4.6, software development).

Compliance with ethical standards

Conflict of interest The authors declare that they have no conflicts of interest.

References

- Bouriaud O, Leban JM, Bert D, Deleuze C (2005) Intra-annual variations in climate influence growth and wood density of Norway spruce. *Tree Physiol* 25:651–660
- Bräuning A, Volland-Voigt F, Burchardt I, Ganzhi O, Nauss T, Peters T (2009) Climatic control of radial growth of *Cedrela montana* in a humid mountain rainforest in southern Ecuador. *Erdkunde* 63:337–345
- Camarero JJ, Guerrero-Campo J, Gutiérrez E (1998) Tree-ring growth and structure of *Pinus uncinata* and *Pinus sylvestris* in the central Spanish Pyrenees. *Arct Antarct Alp Res* 30:1–10
- Deslauriers A, Morin H (2005) Intra-annual tracheid production in balsam fir stems and the effect of meteorological variables. *Trees Struct Funct* 19:402–408
- Deslauriers A, Morin H, Urbinati C, Carrer M (2003) Daily weather response of balsam fir (*Abies balsamea* (L.) Mill.) stem radius

- increment from dendrometer analysis in the boreal forests of Québec (Canada). *Trees Struct Funct* 17:477–484
- Deslauriers A, Rossi S, Anfodillo T (2007) Dendrometer and intra-annual tree growth: what kind of information can be inferred? *Dendrochronologia* 25:113–124
- Duchesne L, Houle D, D'Orangeville L (2012) Influence of climate on seasonal patterns of stem increment of balsam fir in a boreal forest of Québec, Canada. *Agric For Meteorol* 162–163:108–114
- Gruber A, Zimmermann J, Wieser G, Oberhuber W (2009) Effects of climate variables on intra-annual stem radial increment in *Pinus cembra* (L.) along the alpine treeline ecotone. *Ann For Sci* 66:503
- Gruber A, Strobl S, Veit B, Oberhuber W (2010) Impact of drought on the temporal dynamics of wood formation in *Pinus sylvestris*. *Tree Physiol* 30:490–501
- Hosoo Y, Yoshida M, Imai T, Okuyama T (2002) Diurnal difference in the amount of immunogold-labeled glucomannans detected with field emission scanning electron microscopy at the innermost surface of developing secondary walls of differentiating conifer tracheids. *Planta* 215:1006–1012
- Irvine J, Grace J (1997) Continuous measurements of water tensions in the xylem of trees based on the elastic properties of wood. *Planta* 202:455–461
- Jiang Y, Wang B, Dong M, Huang Y, Wang M, Wang B (2015) Response of daily stem radial growth of *Platycladus orientalis* to environmental factors in a semi-arid area of north China. *Trees Struct Funct* 29:87–96
- King G, Fonti P, Nievergelt D, Büntgen U, Frank D (2013) Climatic drivers of hourly to yearly tree radius variations along a 6 °C natural warming gradient. *Agric For Meteorol* 168:36–46
- Körner C, Paulsen J (2004) A world-wide study of high altitude treeline temperatures. *J Biogeogr* 31:713–732
- Lapointe-Garant MP, Huang JG, Gea-Izquierdo G, Raulier F, Bernier P, Berninger F (2010) Use of tree rings to study the effect of climate change on trembling aspen in Québec. *Glob Change Biol* 16:2039–2051
- Li J, Chen F, Cook ER, Gou X, Zhang Y (2007) Drought reconstruction for north central China from tree rings: the value of the Palmer drought severity index. *Int J Climatol* 27:903–909
- Li X, Liang E, Gričar J, Prisljan P, Rossi S, Čufar K (2013) Age dependence of xylogenesis and its climatic sensitivity in Smith fir on the south-eastern Tibetan Plateau. *Tree Physiol* 33:48–56
- Li X, Liang E, Gričar J, Rossi S, Čufar K, Ellison AM (2017) Critical minimum temperature limits xylogenesis and maintains treelines on the southeastern Tibetan Plateau. *Sci Bull* 62:804–812
- Liang E, Shao X, Eckstein D, Huang L, Liu X (2006) Topography- and species-dependent growth responses of *Sabina przewalskii* and *Picea crassifolia* to climate on the northeast Tibetan Plateau. *For Ecol Manag* 236:268–277
- Liang E, Eckstein D, Shao X (2009) Seasonal cambial activity of relict Chinese pine at the northern limit of its natural distribution in north China—exploratory results. *IAWA J* 30:371–378
- Liu Y, Ma L, Leavitt SW, Cai Q, Liu W (2004) Seasonal precipitation reconstruction from tree-ring stable carbon isotope for Mt. Helan, China since AD 1800. *Glob Planet Change* 41:229–239
- Liu Z, Wang Y, Tian A, Yu P, Xiong W, Xu L, Wang Y (2017) Intra-annual variation of stem radius of *Larix principis-rupprechtii* and its response to environmental factors in Liupan Mountains of northwest China. *Forests* 8:382
- Maaten EVD (2013b) Thinning prolongs growth duration of European beech (*Fagus sylvatica* L.) across a valley in southwestern Germany. *For Ecol Manag* 306:135–141
- Maaten EVD, Bouriaud O, Maaten-Theunissen MVD, Mayer H, Spiecker H (2013a) Meteorological forcing of day-to-day stem radius variations of beech is highly synchronic on opposing aspects of a valley. *Agric For Meteorol* 181:85–93
- Major JE, Johnsen KH (2001) Shoot water relations of mature black spruce families displaying a genotype × environment interaction in growth rate. III. Diurnal patterns as influenced by vapor pressure deficit and internal water status. *Tree Physiol* 21:579–587
- Mäkinen H, Seo JW, Nöjd P, Schmitt U, Jalkanen R (2008) Seasonal dynamics of wood formation: a comparison between pinning, microcoring and dendrometer measurements. *Eur J For Res* 127:235–245
- Moser L, Fonti P, Büntgen U, Esper J, Luterbacher J, Franzen J, Frank D (2010) Timing and duration of European larch growing season along altitudinal gradients in the Swiss Alps. *Tree Physiol* 30:225–233
- Murray FW (1967) On the computation of saturation vapor pressure. *J Appl Meteorol* 6:203–204
- Pinheiro JC, Bates DM (2001) Mixed-effects models in S and S-Plus. *J Am Stat Assoc* 96:1135–1136
- R Core Team (2012) R: a language and environment for statistical computing. R Foundation for Statistical Computing, Vienna
- Ren P, Rossi S, Camarero JJ, Ellison AM, Liang E, Peñuelas J (2017) Critical temperature and precipitation thresholds for the onset of xylogenesis of *Juniperus przewalskii* in a semi-arid area of the north-eastern Tibetan Plateau. *Ann Bot* 121:617–624
- Rossi S, Deslauriers A, Anfodillo T, Morin H, Saracino A, Motta R, Borghetti M (2006) Conifers in cold environments synchronize maximum growth rate of tree-ring formation with day length. *New Phytol* 170:301–310
- Rossi S, Deslauriers A, Anfodillo T, Carraro V (2007) Evidence of threshold temperatures for xylogenesis in conifers at high altitudes. *Oecologia* 152:1–12
- Rossi S, Deslauriers A, Gričar J, Seo JW, Rathgeber CBK, Anfodillo T, Morin H, Levanic T, Oven P, Jalkanen R (2008) Critical temperatures for xylogenesis in conifers of cold climates. *Glob Ecol Biogeogr* 17:696–707
- Schweingruber FH (1996) Tree-rings and environment: dendroecology. Birmensdorf, Haupt
- Shishov VV, Tychkov II, Popkova MI, Ilyin VA, Bryukhanova MV, Kirdyanov AV (2016) VS-oscilloscope: a new tool to parameterize tree radial growth based on climate conditions. *Dendrochronologia* 39:42–50
- Sun J, Liu Y (2015) Age-independent climate-growth response of Chinese pine (*Pinus tabulaeformis* Carrière) in North China. *Trees Struct Funct* 29:397–406
- Swidrak I, Gruber A, Kofler W, Oberhuber W (2011) Effects of environmental conditions on onset of xylem growth in *Pinus sylvestris* under drought. *Tree Physiol* 31:483–493
- Tardif J, Flannigan M, Bergeron Y (2001) An analysis of the daily radial activity of 7 boreal tree species, northwestern Quebec. *Environ Monit Assess* 67:141–160
- Tian Q, He Z, Xiao S, Peng X, Ding A, Lin P (2017) Response of stem radial growth of Qinghai spruce (*Picea crassifolia*) to environmental factors in the Qilian Mountains of China. *Dendrochronologia* 44:76–83
- Urrutia-Jalabert R, Rossi S, Deslauriers A, Malhi Y, Lara A (2015) Environmental correlates of stem radius change in the endangered *Fitzroya cupressoides* forests of southern Chile. *Agric For Meteorol* 200:209–221
- Vaganov EA, Hughes MK, Shashkin AV (2006) Growth dynamics of conifer tree rings. Springer, Berlin
- Vieira J, Rossi S, Campelo F, Freitas H, Nabais C (2013) Seasonal and daily cycles of stem radial variation of *Pinus pinaster* in a drought-prone environment. *Agric For Meteorol* 180:173–181
- Wang Z, Bao Y, Deslauriers A, Bräuning A (2015) Intra-annual stem radial increment response of Qilian juniper to temperature and precipitation along an altitudinal gradient in northwestern China. *Trees Struct Funct* 29:25–34

- Wang W, Zhang F, Yuan L, Wang Q, Zheng K, Zhao C (2016) Environmental factors effect on stem radial variations of *Picea crassifolia* in Qilian Mountains, northwestern China. *Forests* 7:210
- Yang B, He M, Shishov V, Tychkov I, Vaganov E, Rossi S, Ljungqvist FC, Bräuning A, Griebinger J (2017) New perspective on spring vegetation phenology and global climate change based on Tibetan Plateau tree-ring data. *Proc Natl Acad Sci USA* 114:6966–6971
- Zeng Q, Rossi S, Yang B (2018) Effects of age and size on xylem phenology in two conifers of northwestern China. *Front Plant Sci* 8:2264
- Zhang L, Jiang Y, Zhao S, Dong M, Chen HYH, Kang X (2016a) Different responses of the radial growth of conifer species to increasing temperature along altitude gradient: *Pinus tabulaeformis* in the Helan Mountains (Northwestern China). *Pol J Ecol* 64:509–525
- Zhang R, Yuan Y, Gou X, Zhang T, Zou C, Ji C, Fan Z, Qin L, Shang H, Li X (2016b) Intra-annual radial growth of Schrenk spruce (*Picea schrenkiana* Fisch. et Mey) and its response to climate on the northern slopes of the Tianshan Mountains. *Dendrochronologia* 40:36–42
- Zweifel R, Häsler R (2000) Frost-induced reversible shrinkage of bark of mature subalpine conifers. *Agric For Meteorol* 102:213–222
- Zweifel R, Zimmermann L, Newbery DM (2005) Modeling tree water deficit from microclimate: an approach to quantifying drought stress. *Tree Physiol* 25:147–156
- Zweifel R, Zimmermann L, Zeugin F, Newbery DM (2006) Intra-annual radial growth and water relations of trees: implications towards a growth mechanism. *J Exp Bot* 57:1445–1459

Publisher's Note Springer Nature remains neutral with regard to jurisdictional claims in published maps and institutional affiliations.